been synthesized in self-assembly systems whose components generate in effect a redox potential that sets the oxidation state of the product cluster. This behavior is delicately balanced for double-cubanes **1**–**3** whose redox potentials (–0.2 to –0.8 V[16,17]) are easily reached, and more than one cluster may be obtained from very similar assembly systems. Because the sulfur atoms of Fe_3S_4 are derived from the $[MS_4]^{z-}$ reactant and require (at least) one M–S bond rupture, the concept of this unit as a ligand is unconventional because it is not obviously preformed prior to incorporation of the heterometal. However, in reaction 4 (Figure 6) this is not the case with protein-bound cuboidal cluster **10**, which binds the indicated metal ions. While there is no crystallographic proof, spectroscopic features of the products indicate the incorporation of the metals into a cluster structure, very likely **11**.[11-15] As shown elsewhere,[15] the structure of **11**-Ni must resemble that of the cubane cluster **9**. The latter cluster was prepared by the reaction of linear $[Fe_3S_4(SEt)_4]^{3-}$ and $Ni(PPh_3)_3$.[15] In this case, the putative ligand is generated by a reductive isomerization.

The only other process involving a preformed cuboidal cluster as a ligand is reaction 5, in which the precursors contain the $[Mo_3S_4]^{4+}$ core **12**. Reduction to the $[Mo_3S_4]^{3+}$ or lower oxidation state is required for incorporation of the heterometal, which affords the structurally proven cubane-type clusters **13**.[49-51] One of these contains the $[Mo_3FeS_4]^{4+}$ core,[49a] with a metal site population that is the inverse of clusters such as **5**. Similarity, reaction 4 succeeds only if the $[Fe_3S_4]^+$ oxidation state is reduced with dithionite. The need for reduction in both cases appear to be analogous. It is probable that the sulfur atoms are not sufficiently electron-rich and polarizable to bind other metals when subjected to the demands of three highly electrophilic Fe^{3+} or Mo^{4+} atoms. Consequently, *reduced* Fe_3S_4 units such as those demonstrated in series **7**–**9** would appear to be essential to the tight incorporation of a M^{z+} heterometal in a cubane structure, regardless of the method of synthesis. We propose that the Fe_3S_4 unit be considered a *quasi-rigid cluster ligand*, whose effective oxidation state lies between 0 and 1– when bound to a fourth metal atom and whose internal structural features and electronic distributions are largely unchanged upon binding of a heterometal atom. A similar description applies to the Mo_3S_4 unit.

Current efforts are directed toward the extension of the synthetic MFe_3S_4 series, including biological metals,[15] and means of stabilization of the voided-cubane structure **10** outside a protein matrix.

Acknowledgment. This research was supported by NIH Grant GM 28856. X-ray equipment was obtained through NIH Grant 1 S10 RR 02247. We thank Dr. G. C. Papaefthymiou for use of a Mössbauer spectrometer and useful discussions.

Supplementary Material Available: For $(Et_4N)[ReFe_3S_4(SEt)_4(dmpe)]$, tables of crystallographic data, intensity collection and structure refinement parameters, positional and thermal parameters, and calculated hydrogen atom positions and a figure of the two independent clusters (11 pages); a listing of observed and calculated structure factors (37 pages). Ordering information is given on any current masthead page.

---

(49) (a) Shibahara, T.; Akashi, H.; Kuroya, H. *J. Am. Chem. Soc.* **1986**, *108*, 1342; *J. Coord. Chem.* **1988**, *18*, 233. (b) Shibahara, T.; Akashi, H.; Kuroya, H. *J. Am. Chem. Soc.* **1988**, *110*, 3313. (c) Akashi, H.; Shibihara, T. *Inorg. Chem.* **1989**, *28*, 2906.

(50) (a) Deeg, A.; Keck, H.; Kruse, A.; Kuchen, W.; Wunderlich, H. *Z. Naturforsch.* **1988**, *43b*, 1541. (b) Keck, H.; Kruse, A.; Mootz, D.; Wiskemann, R.; Wunderlich, H. *Z. Naturforsch.* **1990**, *45b*, 508.

(51) Wu, X.; Lu, S.; Zu, L.; Wu, Q.; Lu, J. *Inorg. Chim. Acta* **1987**, *133*, 39.

Contribution from the Department of Chemistry and Laboratory for Molecular Structure
and Bonding, Texas A&M University, College Station, Texas 77843

Synthesis and Characterization of $Mo_2(OC_6F_5)_4(PMe_3)_4$

F. A. Cotton* and K. J. Wiesinger

Received August 2, 1990

The synthesis and molecular structure of $Mo_2(OC_6F_5)_4(PMe_3)_4$ (**1**) are reported. The synthesis involves the alcoholysis of $Mo_2(CH_3)_4(PMe_3)_4$ by C_6F_5OH to form **1** and $CH_4(g)$. Compound **1** adopts a structural type that has not yet been seen for $Mo_2X_4L_4$ species. Crystal data for **1** are as follows: space group $P\bar{1}$, a = 11.368 (3) Å, b = 13.094 (3) Å, c = 10.574 (2) Å, α = 109.30 (2)°, β = 107.26 (2)°, γ = 95.01 (2)°, V = 1388 (1) Å^3, and Z = 1.

Introduction

For a molecule of the composition $M_2X_4L_4$, with a multiply bonded M_2 unit, a number of isomers are possible. By employment of a numbering scheme that was briefly mentioned in an earlier paper,[1] these isomers may be systematically and rigorously enumerated. The numbering scheme for a square-prismatic structure with a vertical M_2 axis is shown in Figure 1, along with a list of $M_2X_4L_4$ isomers. Pairs of isomers coupled by braces are enantiomorphs.

There are altogether ten geometric isomers, three of which are chiral and include enantiomorphs, to give a total of thirteen. Of these, four have unequal numbers of each kind of ligand at each end, viz., 4 vs 0 or 3 vs 1. In this group there is but one example of the 1,2,3,4-type. No example of any 3 vs 1 type has been reported.

Of the remaining six types of geometrical isomers, four have been observed. The 1,3,6,8-type is overwhelmingly the most common, and all the $Mo_2X_4(PR_3)_4$ molecules with X = halide,[2] CH_3,[3] NCS,[4] and NCO[4] are of this type. It is doubtless favored in these cases by the simple steric effect of the large PR_3 ligands avoiding adjacent positions. This tendency of the larger neutral ligands to occupy alternate vertices can be overcome by the use of bi- or multidentate ligands, thus allowing the isolation of species with (1,2,5,8/1,2,6,7), (1,2,7,8), and (1,3,5,7) distributions.

In this paper we report the first example of a 1,2,7,8 isomer in which all ligands are unidentate, namely $Mo_2(OC_6F_5)_4(PMe_3)_4$. A few other $M_2X_4L_4$ species in which X is an alkoxide have previously been reported, namely those listed in Table I. Five

---

* To whom correspondence should be addressed.

(1) Cotton, F. A.; Price, A. C.; Vidyasagar, K. *Inorg. Chem.* **1990**, *29*, 5143.

(2) Cotton, F. A.; Walton, R. A. *Multiple Bonds Between Metal Atoms*; John Wiley & Sons: New York, 1982.

(3) (a) Cotton, F. A.; Wiesinger, K. J. *Inorg. Chem.* **1990**, *29*, 2594. (b) Girolami, G. S.; Mainz, V. V.; Andersen, R. A.; Vollmer, S. H.; Day, V. W. *J. Am. Chem. Soc.* **1981**, *103*, 3953. (c) Andersen, R. A.; Jones, R. A.; Wilkinson, G. *J. Chem. Soc., Dalton Trans.* **1978**, 446.

(4) Cotton, F. A.; Matusz, M. *Inorg. Chem.* **1988**, *27*, 2127.

(5) Chisholm, M. H.; Folting, K.; Huffman, J. C.; Tatz, R. J. *J. Am. Chem. Soc.* **1984**, *106*, 1153.

(6) Coffindaffer, T. W.; Niccolai, G. P.; Powell, D.; Rothwell, I. P.; Huffman, J. C. *J. Am. Chem. Soc.* **1985**, *107*, 3572.

0020-1669/91/1330-0750$02.50/0

Table I. Structural Features for the Alkoxide Species of the Mo_2^{4+} Core

no.	compd	bond dist, Å Mo–Mo	Mo–O	Mo–N/P	ref
1	$Mo_2(OC_6F_5)_4(PMe_3)_4$	2.146 (2)	2.09 [2]	2.62 (5)	this work
2	$Mo_2(O\text{-}i\text{-}Pr)_4(py)_4$	2.195 (1)	2.03 (1)	2.27 (1)	5
3	$Mo_2(OCH_2\text{-}t\text{-}Bu)_4(HNMe_2)_4$	2.133 (2)	2.08 (1)	2.27 (2)	5
4	$Mo_2(OCH_2\text{-}t\text{-}Bu)_4(PMe_3)_4$	2.209 (1)	2.03 (2)	2.54 (2)	5
5	$Mo_2(O\text{-}i\text{-}Pr)_4(HO\text{-}i\text{-}Pr)_4$	2.110 (3)	2.09 (1) (OR) 2.17 (1) (HOR)		5
6	$Mo_2(O\text{-}i\text{-}Pr)_4(dmpe)_4$	2.236 (1)	2.00 (1)	2.438 (1)	8
7	$Mo_2(OC_6F_5)_4(HNMe_2)_4$	2.140 (2)	2.07 (1)	2.24 (1)	7

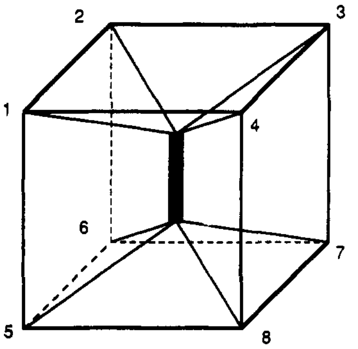

3 or 4 like ligands on each end:
*a 1,2,3,4
{1,2,3,5 1,2,3,7} 1,2,3,6 1,2,3,8
others:
1,2,5,6 {1,2,5,7 1,2,6,8}
*b {1,2,5,8 1,2,6,7}
*c 1,2,7,8
*d 1,3,5,7
*e 1,3,6,8

[a] Only one example with chelating dmpe ligands

[b] Only one example with a tetradentate ligand, $R_2P\text{-}P(R)\text{-}P(R)\text{-}PR_2$. F. A. Cotton and J. -D. Chen, unpublished results.

[c] Previously known only with two bidentate ligands, e.g., $\alpha\text{-}Mo_2X_4(dppe)_2$.

[d] Known both with bidentate ligands, e.g., $\beta\text{-}M_2X_4(dppe)_2$, and with unidentate ligands, e.g., $Mo_2Br_4(pic)_4$; see text.

[e] many examples; see text.

Figure 1. Possible isomers for $M_2X_4(L)_4$ molecules. Those marked by asterisks are known.

of these, **2**–**5** and **7**, have the 1,3,6,8 structures, while one, $Mo_2(OCHMe_2)_4(Me_2PCH_2CH_2PMe_2)_2$, constitutes the only prior example of a 1,2,3,4 isomer.

All of the $Mo_2(OR)_4L_4$ compounds previously reported were made by reactions between $Mo_2(NMe_2)_6$ and an alcohol,[9] followed in some cases by addition of a neutral ligand to displace the autogenous $HNMe_2$ ligand, as summarized in the following equations:

$$Mo_2(NMe_2)_6 + C_6F_5OH \rightarrow Mo_2(OC_6F_5)_4(HNMe_2)_4$$

$$Mo_2(i\text{-}Bu)_2(NMe_2)_4 + t\text{-}BuCH_2OH \rightarrow$$

$$Mo_2(OCH_2\text{-}t\text{-}Bu)_4(HNMe_2)_4 + \text{isobutylene} + \text{isobutane}$$

$$\Big\downarrow PMe_3$$

$$Mo_2(OCH_2\text{-}t\text{-}Bu)_4(PMe_3)_4$$

Our goal was to find a practical synthetic route to $Mo_2(OR_F)_4(PR_3)_4$ species (OR_F = fluoroalkoxides) directly from Mo_2^{4+} cores. In light of recent work in our group,[7] it was envisioned that these species might provide new structural types and show how the special electronic properties of the fluoroalkoxides affect the Mo–Mo bond distance. In pursuance of this, reported here is the synthesis and characterization of $Mo_2(OC_6F_5)_4(PMe_3)_4$ (**1**) from the reaction between $Mo_2(CH_3)_4(PMe_3)_4$ and C_6F_5OH, where the elimination of methane provides the driving force for an efficient (>80%) preparative reaction.

Experimental Section

All manipulations were performed under an inert atmosphere of dry and oxygen-free argon. All solvents were predried over molecular sieves, refluxed over NaK at least 24 h, and then freshly distilled under dinitrogen. Glassware was dried at 120 °C for >12 h prior to use.

The phosphines were purchased from Strem, Inc., and used as received. The fluoroalcohols were purchased from Aldrich, Inc., and used as received, unless otherwise noted. The UV–vis data was collected on a Carey 17-D spectrophotometer. $Mo_2(CH_3)_4(PMe_3)_4$ and $Mo_2(CH_3)_4(PMe_2Ph)_4$ were synthesized according to the literature procedure.[3a]

Preparation of Pentafluorophenol Solution. A Schlenk tube equipped with a cold finger was charged with 1.20 g of pentafluorophenol, cooled to 0 °C, and subjected to several pump/fill cycles on the Schlenk line (the cooling is necessary to reduce the volatility of the fluoroalcohol). Sublimation was commenced by heating the Schlenk tube to 35–40 °C, cooling the cold finger to −78 °C, and applying a static vacuum. White needles formed on the cold finger and a cream-colored residue was left behind. The apparatus was taken into a drybox to isolate the pure pentafluorophenol. Pure pentafluorophenol (0.772 g, 4.19 mmol) was placed in a 25-mL volumetric flask and diluted to the mark with a 3:2 mixture of thf/hexane. The resulting solution was transferred to a Schlenk tube. The concentration of the solution was 0.168 M.

Preparation of $Mo_2(OC_6F_5)_4(PMe_3)_4$. $Mo_2(CH_3)_4(PMe_3)_4$ (0.0648 g, 0.116 mmol) was dissolved in hexanes (6 mL) to give a deep blue solution. Benzene (5 mL) was injected beneath the hexane layer, and then the C_6F_5OH solution (2.78 mL, 0.467 mmol) was injected beneath both of the above layers. After 2 weeks, large emerald green crystals were deposited on the sides of the Schlenk tube. The solid can be isolated by decantation of the supernatant liquid. The remaining green solid was washed with hexanes and ether and dried under vacuum. The yield was >80%. The compound is insoluble in common solvents. A UV–vis spectrum (Nujol mull) shows two bands at 658 and 390 nm. A melting point determination led to decomposition at 165 °C.

X-ray Crystallography. The crystals were grown as described above. Upon inspection of the crystals under a blanket of dry, degassed mineral oil, it was discovered that many were not of good quality, especially those taken from the region of the benzene/hexane interface of the crystallizing solution. Several crystals were found that were of appropriate size and extinguished well under polarized light. One of these crystals was mounted on a quartz fiber with epoxy cement. Crystal data and data collection parameters are listed in Table II. The crystal was put on the X-ray machine and optically centered, and 25 reflections were found from three regions of reciprocal space. Centering, indexing, and a least-squares calculation on the 25 reflections gave a triclinic crystal system. The axial photographs confirmed this assignment.

After 3797 reflections were collected, the generator of the CAD-4 burnt out and was replaced. The crystal and all 25 reflections were recentered to obtain the original cell. Some common reflections (480) were recollected and then the rest of the data set was collected. The two data sets were reduced in the same way (see below) and were merged to give R_{merge} = 0.0153 for the set of common reflections.

The data were corrected for absorption by using azimuthal scans of six reflections with an Eulerian angle of χ near 90°. No decay correction was used. The ambiguity between the space groups $P1$ and $P\bar{1}$ was resolved by a successful refinement in $P\bar{1}$. A Patterson synthesis revealed the disordered molybdenum atoms. By employment of alternating difference Fourier maps and least-squares refinements, the whole molecule was obtained. A thf solvent molecule was found and determined to be disordered over two positions. The program SHELX-76 was used to refine

---

(7) Abbott, R. G.; Cotton, F. A.; Falvello, L. R. *Inorg. Chem.* **1990**, *29*, 514.

(8) Chisholm, M. H.; Huffman, J. C.; Van Der Sluys, W. G. *J. Am. Chem. Soc.* **1987**, *109*, 2514.

(9) Chisholm, M. H.; Haitko, D. A.; Murillo, C. A. *Inorg. Synth.* **1982**, *21*, 51.

Table II. Crystal Data for $Mo_2(OC_6F_5)_4(PMe_3)_4{\cdot}2thf$ (**1**)

formula	$Mo_2P_4F_{20}O_6C_{44}H_{52}$
fw	1372.65
space group	$P\bar{1}$
a, Å	11.368 (3)
b, Å	13.094 (3)
c, Å	10.574 (2)
α, deg	109.30 (2)
β, deg	107.26 (2)
γ, deg	95.01 (2)
V, Å^3	1388 (1)
Z	1
d_{calc}, g/cm^3	1.642
crys size, mm	0.61 × 0.30 × 0.19
μ(Mo Kα), cm^{-1}	6.554
data colln instrument	Enraf-Nonius CAD-4
radiation monochromated in incident beam (λ, Å)	Mo Kα (0.71073)
orientation reflcns: no.; range (2θ), deg	25; $21 < 2\theta < 38$
temp, °C	22
scan method	ω
data colln range (2θ), deg	$4 \leq 2\theta \leq 50$
no. of unique data; tot. no. with $F_o^2 > 3\sigma(F_o^2)$	4339; 2830
no. of params refined	312
transm factors: max; min	1.00; 0.91
R^a	0.0592
$R_w^{\,b}$	0.0782
quality-of-fit indicator[c]	1.645
largest shift/esd, final cycle	0.03
largest peak, e/Å^3	0.551

[a] $R = \sum||F_o| - |F_c||/\sum|F_o|$. [b] $R_w = [\sum w(|F_o| - |F_c|)^2/\sum w|F_o|^2]^{1/2}$; $w = 1/\sigma^2(|F_o|)$. [c] Quality-of-fit $= [\sum w(|F_o| - |F_c|)^2/(N_{observns} - N_{params})]^{1/2}$.

the molybdenum and thf disorder, which resulted in disorders of 56:44 and 55:45, respectively. Assignments of the oxygen atoms in the thf ring were purely arbitrary. The *x*, *y*, and *z* coordinates of the thf molecule were fixed, and only their multiplicities and a common thermal parameter for each thf ring were allowed to refine freely. Final residuals and figures of merit are reported in Table II. Selected bond distances and bond angles are listed in Table III. Positional and equivalent isotropic thermal parameters are listed in Table IV.

Results and Discussion

Synthesis and Physical Properties. A bright blue hydrocarbon solution of $Mo_2(CH_3)_4(PMe_3)_4$ reacts immediately at room temperature with C_6F_5OH to give an emerald green solution and a noticeable evolution of gas (CH_4).

$$Mo_2Me_4(PMe_3)_4 + 4C_6F_5OH \rightarrow Mo_2(OC_6F_5)_4(PMe_3)_4 + 4CH_4(g)$$

Within minutes, the green solution forms a fine colloidial suspension from which an emerald green solid precipitates over the course of several hours. The emerald green solid is stable in air for weeks and resistant to attack by ethanol/HNO_3 solution for >5 days but decomposes at 165 °C with a release of PMe_3 (as detected by a distinct odor during a melting point determination).

A UV-vis spectrum (Nujol mull) of $Mo_2(OC_6F_5)_4(PMe_3)_4$ reveals bands at 658 and 390 nm, which are similar to those reported for $Mo_2(3,5\text{-}Me_2\text{-}C_6H_3O)_4(PMe_3)_4$.[6] A ^1H NMR experiment was attempted by allowing the reaction to occur in an NMR tube (C_6D_6) and immediately obtaining a spectrum. The rapid formation of the solid material, even when very dilute solutions are employed, prevented the assignment of peaks. Several sets of peaks were seen in the PMe_3 region and indicated that many intermediates were present in solution. The Mo-Me resonance at −0.482 ppm[3a] had disappeared. An emerald green solid precipitated over several hours to leave a clear solution, which showed no peaks in the ^1H NMR spectrum. We conclude that while there are may species present in solution, the final product $[Mo_2(OC_6F_5)_4(PMe_3)_4]$ cannot be observed because of its rapid precipitation from solution.

The insolubility of 1,2,7,8-$Mo_2(OC_6F_5)_4(PMe_3)_4$ leaves open the question of whether this is really the most stable (thermodynamically) isomer, rather than, perhaps, the 1,3,6,8 isomer obtained for $Mo_2(OC_6F_5)_4(HNMe_2)_4$.[7] Of course, it may be, but the possibility that it is obtained only because its insolubility makes it the most stable solid phase (as opposed to the preferred molecular structure) cannot be ruled out.

Other reactions have been performed with $Mo_2Me_4L_4$ (L = PMe_3, PMe_2Ph) and the fluoroalcohols C_6F_5OH, CF_3CH_2OH, and $(CF_3)_2C(H)OH$. In all these reactions, the solutions turned emerald green and then proceeded to form green or brown products. Unfortunately, all attempts to obtain crystals, by various techniques, have been unsuccessful. The green solutions exhibit spectral characteristics in the UV-vis region similar to those seen for **1**.

Molecular Structure. The title compound crystallizes in the space group $P\bar{1}$. The molecule resides on an inversion center. Selected bond distances and angles are shown in Table III. The molecular structure is shown in Figure 2. The Mo-Mo bond distance is 2.146 (2) Å, which is consistent with other quadruply bonded dimolybdenum systems.[2] The Mo-P bond lengths are

Table III. Selected Bond Distances (Å) and Bond Angles (deg) for $Mo_2(OC_6F_5)_4(PMe_3)_4{\cdot}2thf$ (**1**)[a]

		Bond Distances			
Mo(1)-Mo(1)′	2.144 (2)	Mo(1)-P(1)	2.640 (2)	Mo(1)-P(2)	2.584 (3)
Mo(2)-Mo(2)′	2.149 (2)	Mo(2)-P(1)′	2.667 (3)	Mo(2)-P(2)′	2.605 (3)
Mo(1)-O(1)	2.136 (5)	Mo(1)-O(2)	2.055 (6)		
Mo(2)-O(1)	2.055 (5)	Mo(2)-O(2)	2.117 (5)		
P(1)-C(1)	1.825 (12)	P(1)-C(2)	1.837 (13)	P(1)-C(3)	1.821 (10)
P(2)-C(4)	1.826 (12)	P(2)-C(5)	1.849 (9)	P(2)-C(6)	1.849 (12)
O(1)-C(7)	1.299 (10)	O(2)-C(13)	1.292 (11)		
		Bond Angles			
Mo(1)′-Mo(1)-P(1)	95.78 (8)	Mo(1)′-Mo(1)-P(2)	95.26 (9)	Mo(2)′-Mo(2)-P(1)′	94.2 (1)
Mo(2)′-Mo(2)-P(2)′	93.99 (9)	Mo(1)′-Mo(1)-O(1)	108.1 (2)	Mo(1)′-Mo(1)-O(2)	113.8 (2)
Mo(2)′-Mo(2)-O(1)	113.5 (2)	Mo(2)′-Mo(2)-O(2)	109.4 (2)	P(1)-Mo(1)-P(2)	87.93 (9)
P(1)′-Mo(2)-P(2)′	86.91 (9)	P(1)-Mo(1)-O(1)	155.9 (2)	P(1)-Mo(1)-O(2)	82.4 (2)
P(2)-Mo(1)-O(1)	86.5 (2)	P(2)-Mo(1)-O(2)	150.1 (2)	P(1)′-Mo(2)-O(1)	82.1 (2)
P(1)′-Mo(2)-O(2)	156.1 (2)	P(2)′-Mo(2)-O(1)	151.0 (2)	P(2)′-Mo(2)-O(2)	87.9 (2)
O(1)-Mo(2)-O(2)	91.5 (2)	O(1)-Mo(1)-O(2)	90.9 (2)		
Mo(1)-P(1)-C(1)	103.4 (3)	Mo(1)-P(1)-C(2)	134.7 (4)	Mo(1)-P(1)-C(3)	112.7 (3)
Mo(2)-P(1)′-C(1)′	135.8 (3)	Mo(2)-P(1)′-C(2)′	99.7 (3)	Mo(2)-P(1)′-C(3)′	113.8 (3)
Mo(1)-P(2)-C(4)	98.8 (4)	Mo(1)-P(2)-C(5)	118.8 (4)	Mo(1)-P(2)-C(6)	128.5 (3)
Mo(2)-P(2)′-C(4)′	132.9 (4)	Mo(2)-P(2)′-C(5)′	116.7 (4)	Mo(2)-P(2)′-C(6)′	95.1 (4)
C(1)-P(1)-C(2)	100.2 (6)	C(1)-P(1)-C(3)	101.1 (5)	C(2)-P(1)-C(3)	99.7 (5)
C(4)-P(2)-C(5)	102.0 (5)	C(4)-P(2)-C(6)	102.3 (5)	C(5)-P(2)-C(6)	101.9 (5)
Mo(1)-O(1)-C(7)	137.7 (4)	Mo(2)-O(1)-C(7)	134.0 (6)		
Mo(1)-O(2)-C(13)	133.2 (6)	Mo(2)-O(2)-C(13)	137.2 (4)		

[a] Numbers in parentheses are estimated standard deviations in the least significant digits.

Table IV. Positional Parameters and Equivalent Isotropic Thermal Parameters (Å^2) and Their Estimated Standard Deviations for $Mo_2(OC_6F_5)_4(PMe_3)_4 \cdot 2thf$ (**1**)

atom	*x*	*y*	*z*	*B*[a]
Mo(1)	0.0529 (1)	0.43570 (9)	0.4912 (1)	3.50 (4)
Mo(2)	−0.0204 (1)	0.5217 (1)	0.4073 (2)	3.61 (5)
P(1)	−0.0837 (2)	0.3124 (2)	0.2234 (3)	6.18 (8)
P(2)	0.2055 (2)	0.5204 (2)	0.3964 (3)	6.04 (8)
O(3)	0.471	0.050	0.144	17.0 (6)*
C(19)	0.339	0.078	0.107	17.0 (6)*
C(20)	0.272	0.043	0.199	17.0 (6)*
C(21)	0.357	−0.019	0.278	17.0 (6)*
C(22)	0.474	−0.025	0.231	17.0 (6)*
O(4)	0.298	−0.052	0.120	12.5 (6)*
C(23)	0.297	0.069	0.134	12.5 (6)*
C(24)	0.415	0.144	0.263	12.5 (6)*
C(25)	0.484	0.068	0.332	12.5 (6)*
C(26)	0.406	−0.052	0.251	12.5 (6)*
F(1)	0.4472 (5)	0.4614 (5)	0.7015 (6)	7.5 (2)
F(2)	0.5768 (5)	0.3620 (5)	0.8643 (7)	9.3 (3)
F(3)	0.4761 (6)	0.2849 (5)	1.0259 (6)	9.7 (3)
F(4)	0.2386 (6)	0.3065 (5)	1.0157 (5)	8.1 (2)
F(5)	0.1076 (4)	0.4063 (4)	0.8563 (5)	6.0 (2)
F(6)	0.1939 (5)	0.2427 (4)	0.4856 (5)	7.0 (2)
F(7)	0.2922 (7)	0.0928 (6)	0.5815 (7)	10.4 (3)
F(8)	0.1815 (8)	−0.0011 (5)	0.7229 (7)	11.9 (3)
F(9)	−0.0305 (8)	0.0564 (6)	0.7617 (8)	12.2 (4)
F(10)	−0.1338 (7)	0.2015 (5)	0.6602 (7)	9.4 (3)
O(1)	0.2083 (5)	0.4837 (4)	0.6865 (5)	5.0 (2)
O(2)	−0.0224 (5)	0.3042 (4)	0.5276 (6)	5.3 (2)
C(1)	−0.002 (1)	0.1988 (9)	0.180 (1)	8.5 (4)
C(2)	−0.128 (1)	0.3349 (9)	0.054 (1)	9.0 (5)
C(3)	−0.2349 (8)	0.2386 (8)	0.205 (1)	7.4 (4)
C(4)	0.2968 (9)	0.4122 (9)	0.369 (1)	7.5 (4)
C(5)	0.2388 (9)	0.6438 (9)	0.522 (1)	8.5 (4)
C(6)	0.1694 (9)	0.5440 (9)	0.227 (1)	7.5 (4)
C(7)	0.2702 (7)	0.4366 (6)	0.7681 (8)	4.4 (2)
C(8)	0.3915 (8)	0.4239 (7)	0.7793 (9)	5.4 (3)
C(9)	0.4598 (8)	0.3728 (8)	0.862 (1)	6.1 (3)
C(10)	0.4109 (9)	0.3341 (8)	0.943 (1)	6.3 (3)
C(11)	0.2918 (9)	0.3463 (7)	0.9392 (8)	5.5 (3)
C(12)	0.2232 (8)	0.3971 (6)	0.8570 (8)	4.8 (3)
C(13)	0.0251 (9)	0.2298 (6)	0.5694 (8)	5.1 (3)
C(14)	0.134 (1)	0.1972 (7)	0.5529 (9)	5.9 (3)
C(15)	0.186 (1)	0.1183 (9)	0.601 (1)	7.6 (4)
C(16)	0.131 (1)	0.0725 (9)	0.672 (1)	8.2 (4)
C(17)	0.022 (1)	0.1016 (9)	0.690 (1)	7.6 (4)
C(18)	−0.027 (1)	0.1752 (8)	0.637 (1)	6.8 (4)

[a] Starred *B* values are for atoms that were refined isotropically. Anisotropically refined atoms are given in the form of the equivalent isotropic displacement parameter defined as $(4/3)[a^2\beta_{11} + b^2\beta_{22} + c^2\beta_{33} + ab(\cos\gamma)\beta_{12} + ac(\cos\beta)\beta_{13} + bc(\cos\alpha)\beta_{23}]$.

typical, and the Mo–O bonds are essentially single bonds as expected[7,10] for OR_F alkoxides.

There is disorder in this structure such that within one resolvable quasi-cubic set of ligands two different pairs of molybdenum atoms are found in nearly equal (56 to 44) proportions. This can be seen from a different perspective in Figure 3, which is a view down one body diagonal of the quasi-cube. Both of these orientations correspond to the same isomeric arrangement of ligands, i.e., 1,2,7,8. The third possible orientation of an Mo_2 unit, orthogonal to these two, is not observed. This is understandable, since it would correspond to a different isomer, 1,3,5,7. Other examples of such an isomer are known[11] (see Figure 1), but in this case, with the large $^-OC_6F_5$ groups, such an isomer is evidently unstable, at least in this crystalline environment, if not intrinsically.

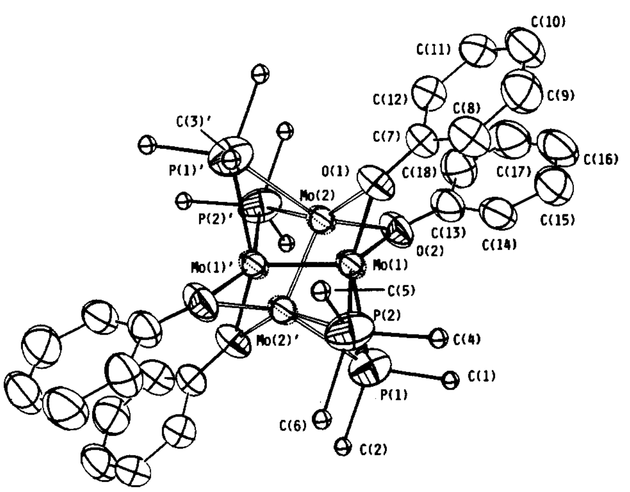

Figure 2. ORTEP drawing of the $Mo_2(OC_6F_5)_4(PMe_3)_4$ (**1**) molecule. The carbon atoms of the trimethylphosphine ligands are represented by spheres of arbitrary radii, and the fluorine atoms are omitted for clarity. Other atoms are represented by their thermal ellipsoids at the 50% probability level. The second pair of disordered molybdenum atoms are represented by the dotted ellipsoids.

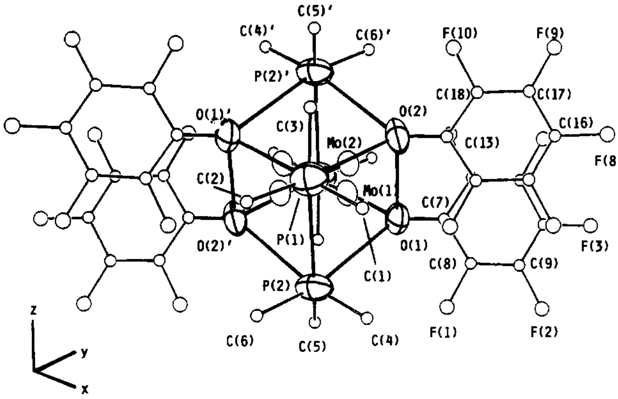

Figure 3. ORTEP drawing of the $Mo_2(OC_6F_5)_4(PMe_3)_4$ (**1**) molecule. The molybdenum, phosphorus, and oxygen atoms are represented by their thermal ellipsoids at the 50% probability level. Other atoms are represented by circles of arbitrary radii. The view is down the P(1)–P(1)′ axis.

While the occurrence of a nearly 1:1 disorder of the Mo_2 units is rather easily explained, failure to observe disorder in the ligands requires some comment. Actually, there is no problem as far as the alkoxide ligands are concerned. Relative to the direction defined by the C–O bond, the oxygen atom may form an additional bond in any direction lying on a cone, and both of the molybdenum atoms adjacent to each oxygen atom may be considered to be on (and indeed define) such a cone. It is the PMe_3 ligands that pose something of a problem.

It is typical in complexes of this type for one carbon atom of the PMe_3 to be pointed away from the Mo–Mo bond (distal)[3a] so that this P–C vector is roughly parallel to the Mo–Mo vector. The other two carbons are then located over the Mo–Mo bond (proximal). In complex **1** the arrangement and symmetry of the system allow for one set of carbon atoms on each phosphorus atom to fulfill the above requirements for both the observed orientations. For example, consider the carbons off of P(1). For the Mo(1)–Mo(1)′ (*x* axis) orientation, C(1) serves as the distal carbon such that the P(1)–C(1) vector is parallel to the Mo(1)–Mo(1)′ vector, while C(2) and C(3) serve as the proximal carbons. For the Mo(2)–Mo(2)′ (*y* axis) orientation, C(2) serves as the distal carbon, while C(1) and C(3) serve as the proximal carbons. It should be noted from Table III that the Mo–P–C angles are normal for C(3) and C(5) but are distorted for C(1), C(2), C(4), and C(6). The normal range for Mo–P–C angles in $Mo_2(X)_4(PMe_3)_4$ structures is 103–115°. Furthermore, the thermal parameters (Table IV) are somewhat larger than typical for the carbon atoms and the phosphorus atoms of PMe_3. As a consequence of the Mo disorder, the electron density for the carbon atoms is really in two different places but too close to be resolved crystallographically.

The observed Mo–O distances for **1** have a mean value, 2.09 [2] Å, that is similar to the value of 2.07 Å predicted for a Mo–O

---

(10) Chisholm, M. H. *Polyhedron* **1983**, *2*, 681.

(11) Brencic, J. V.; Golic, L.; Leban, I.; Segedin, P. *Monatsh. Chem.* **1978**, *17*, 3254.

single bond.[10] In compounds with the Mo_2^{6+} core, the observed terminal Mo–O distance is 1.80–1.96 Å and is a result of the π-bonding component of the Mo–O bond. In our compound, the molybdenum atom, as in other Mo_2^{4+} core complexes, has no vacant d orbitals that can accept π-electron density from the pentafluorophenoxide ligands. A weak Mo–O π bond is possible by the mixing of the oxygen π orbitals with the δ^* and π^* orbitals of the Mo–Mo bond. The latter tends to shorten the Mo–O bond and lengthen the Mo–Mo bond, and indeed, that seems to be the case for compounds **2** and **4** as listed in Table I. Our species appears to contain only a single Mo–O bond without any Mo–O π component. This was expected, since the pentafluorophenoxide ligand has highly electron-withdrawing fluorides, which decrease the amount of electron density available to the oxygen atom's π orbitals.

Conclusions

This report adds two important pieces of information to the literature. First, the coordinatively saturated $Mo_2(CH_3)_4(PMe_3)_4$ species are reactive toward alcoholic species and allow a direct synthetic route to $Mo_2(OC_6F_5)_4(PMe_3)_4$. Second, complex **1** represents the first centrosymmetric [*cis*-$Mo(OR)_2(L)_2]_2$ species that contains all monodentate ligands.

Acknowledgment. We thank the National Science Foundation for support.

Supplementary Material Available: Tables of complete bond distances and angles and general displacement parameter expressions (5 pages); a table of observed and calculated structure factors (16 pages). Ordering information is given on any current masthead page.

Contribution from the Department of Chemistry,
The University of Michigan, Ann Arbor, Michigan 48109-1055

Studies of the Reactivity of Binary Thio- and Tertiary Oxothiomolybdates toward Electrophiles. Reactions with Dicarbomethoxyacetylene and the Synthesis and Structures of the $[Et_4N]_2[MoO(L)_2]$, *anti*-$[Et_4N]_2[Mo_2O_2S_2(L)_2]$, *syn*-$[Ph_4P]_2[Mo_2O_2S_2(L)_2]\cdot 2DMF$, $[Ph_4P]_2[Mo(L)_3]\cdot DMF\cdot C_6H_6$, and $[Ph_4P]_2[Mo_2S_2(L)_4]\cdot 2CH_2Cl_2$ Complexes (L = 1,2-Dicarbomethoxy-1,2-ethylenedithiolate)

D. Coucouvanis,* A. Hadjikyriacou, A. Toupadakis, Sang-Man Koo, O. Ileperuma, M. Draganjac, and A. Salifoglou

Received July 6, 1990

The reactions of various thio- or oxothiomolybdates with the activated alkyne dicarbomethoxyacetylene, DMA, are described. The syntheses of the diamagnetic $[Et_4N]_2[MoO(L)_2]$ (I), *anti*-$[Et_4N]_2[Mo_2O_2S_2(L)_2]$ (II), *syn*-$[Ph_4P]_2[Mo_2O_2S_2(L)_2]\cdot 2DMF$ (III), $[Ph_4P]_2[Mo(L)_3]\cdot DMF\cdot C_6H_6$ (IV), and $[Ph_4P]_2[Mo_2S_2(L)_4]\cdot 2CH_2Cl_2$ (V) complexes (L = 1,2-dicarbomethoxy-1,2-ethylenedithiolate, DMAD) are accomplished in reactions of DMA with $(Et_4N)_2[MoO(S_4)_2]$, $(Et_4N)_2[Mo_2O_2S_9]$, $(Ph_4P)_2[Mo_2OS_7]$, $(Ph_4P)_2[MoS(S_4)_2]$, and $(Ph_4P)_2[Mo_2S_{10}/S_{12}]$, respectively. It is proposed that these reactions proceed by electrophilic attack of DMA on either Mo═S or $Mo–S_2$ with subsequent DMA insertion into these chromophores. The unstable vinyl sulfide or vinyl disulfide intermediates are converted to the final dithiolene products either thermally or by a sulfur-catalyzed pathway. The compounds I–V crystalize in the space groups $P2_1/c$, $P\bar{1}$, $P\bar{1}$, $C2/c$, and $P\bar{1}$, respectively. The cell dimensions are a = 17.664 (4) Å, b = 9.979 (2) Å, c = 21.363 (4) Å, and β = 100.5 (2)° for I, a = 9.004 (2) Å, b = 8.975 (3) Å, c = 13.904 (2) Å, α = 90.53 (2)°, β = 102.04 (1)°, and γ = 112.11 (2)° for II, a = 12.919 (4) Å, b = 14.863 (6) Å, c = 18.844 (6) Å, α = 95.86 (3)°, β = 102.61 (2)°, and γ = 93.74 (3)° for III, a = 22.907 (14) Å, b = 14.619 (9) Å, c = 43.746 (21) Å, and β = 95.34 (5)° for IV, and a = 12.778 (2) Å, b = 13.616 (3) Å, c = 13.898 (3) Å, α = 105.62 (2)°, β = 98.80 (1)°, and γ = 110.10 (1) for V. The data for all structures were obtained on an automatic diffractometer employing Mo Kα radiation. Full-matrix refinement of 393 parameters on 2704 data for I, 217 parameters on 1774 data for II, 775 parameters on 6350 data for III, 389 parameters on 2637 data for IV, and 313 parameters on 2412 data for V gave final R_w values of 0.050, 0.024, 0.044, 0.077, and 0.066, respectively. The structure of I shows the Mo^{IV} coordinated by a terminal oxo ligand and two bidentate DMA ligands in the equatorial plane of the distorted square-pyramidal $Mo^{IV}(O)(S_4)$ core unit (Mo═O = 1.686 (6) Å; $Mo–S_{eq}$ = 2.380 (4) Å). The structures of the *anti*- and *syn*-$[Mo_2O_2(\mu_2\text{-}S)_2]^{2+}$ units in II and III have idealized C_{2h} and C_{2v} geometry, respectively. Each unit is coordinated by two DMAD bidentate ligands. The $Mo^V(O)(S_4)$ subunits are distorted square pyramidal with a terminal oxo ligand and the DMAD and μ_2-S ligands occupying the equatorial planes. Adjacent pyramids share the bridging S ligands as common equatorial sites (for II, Mo–Mo = 2.904 (1) Å, Mo═O = 1.684 (2) Å, $Mo–S_b$ = 2.328 Å, $Mo–S_L$ = 2.419 Å, $Mo–S_b–Mo$ = 77.13 (1)°, and $S_b–Mo–S_b$ = 102.91 (1)°; for III, Mo–Mo = 2.853 (1) Å, Mo═O = 1.675 (2) Å, $Mo–S_b$ = 2.331 (3) Å, $Mo–S_L$ = 2.425 (8) Å, $Mo–S_b–Mo$ = 75.5 (1)°, and $S_b–Mo–S_b$ = 100.9 (1)°). The structure of IV shows the Mo(IV) coordinated by three bidentate DMAD ligands and contains the slightly distorted trigonal prismatic $[Mo^{IV}(S)_6]$ core ($Mo–S_L$ = 2.393 Å). The structure of the centrosymmetric anion in V contains two edge-sharing distorted octahedral $[Mo^V(S)_6]$ units that share the bridging S ligands. The Mo^V in each of these subunits, in addition to the two bridging sulfides, is coordinated by two bidentate DMAD ligands (Mo–Mo = 2.938 Å, $Mo–S_b$ = 2.321 Å, $Mo–S_L$ = 2.383, 2.459 Å; $Mo–S_b–Mo$ = 78.6 (1)°, $S_b–Mo–S_b$ = 101.4 (1)°). The different $Mo–S_L$ bonds in V are attributed to a significant trans effect of the bridging ligands. The spectroscopic and electrochemical properties of these complexes as well as a discussion of the reactivity characteristics of the various Mo-centered functional groups are discussed.

Introduction

In the last decade our understanding of synthetic and structural aspects in the chemistry of the binary Mo/S and tertiary Mo/S/O complexes has reached a relatively advanced level. As a result of extensive synthetic and crystallographic studies in various laboratories, nearly complete series of the $[(L)Mo(E)(\mu\text{-}S)_2Mo(E')(L')]^{2-}$ anions (Figure 1) (E = E′ = S: L = L′ = S;[1] L = S, L′ = S_2;[1] L = L′ = S_2;[2] L = S, L′ = S_4;[1] L = S_2, L′ = S_4;[3]

---

(1) Hadjikyriacou, A. I.; Coucouvanis, D. *Inorg. Chem.* **1987**, *26*, 2400.

0020-1669/91/1330-0754$02.50/0 © 1991 American Chemical Society